Am J Transl Res 2021;13(11):13135-13146
www.ajtr.org /ISSN:1943-8141/AJTR0134482

Original Article

CCR10/CCL27 crosstalk regulates cell metastasis via PI3K-Akt signaling axis in non-small-cell lung cancer

Yonggang Liu[1*], Ailian Xiao[2*], Biyuan Zhang[3]

[1]Department of Thoracic Oncology, Baotou Cancer Hospital, Baotou 014000, Inner Mongolia, China; [2]Department of Respiratory and Critical Care Medicine, General Hospital of TISCO, Taiyuan 030003, Shanxi, China; [3]Department of Radiation Oncology, The affiliated Hospital of Qingdao University, Qingdao 266003, Shandong, China. [*]Equal contributors and co-first authors.

Received April 20, 2021; Accepted July 2, 2021; Epub November 15, 2021; Published November 30, 2021

Abstract: Previous research has shown that CCR10 acts as a vital oncogene in the progression of multiple malignancies. However, its effect on the treatment of non-small-cell lung cancer (NSCLC) has not been investigated. Current research examined the effect of CCR10 on the cellular survival and migration of NSCLC, and the modulation of cell death and found that the expression levels of CCR10 and CCL27 (ligand) were highly upregulated in human NSCLC tissue and cell lines, A549 and H157, compared with adjacent normal lung specimens. MTT and colony formation assays revealed that the blockage of CCR10 inhibited the multiplication and survival of A549 and H157 cells. Further study showed that metastasis-relevant VEGF-C/D, MMP-2/9, TIMP-1/2 were also regulated via CCR10 activation. Notably, increased NF-κB levels were detected in cells with activated CCR10, whereas the levels of NF-κB decreased in cells with blocked CCR10. Finally, the recovery of NF-κB expression counteracted the suppressive influence of CCR10 blockage on NSCLC cell survival, migration, and invasion. These results improved our knowledge understanding the molecular mechanisms of CCR10-CCL27 in progression of NSCLC.

Keywords: Non-small-cell lung cancer, CCR10, CCL27, migration, viability

Introduction

Non-small-cell lung cancer (NSCLC) includes adenocarcinoma (AD) and squamous cell carcinoma (SCC), ranking among the top 10 cancers in prevalence and mortality worldwide. NSCLC is a tumor with high malignancy, rather poor prognosis, and strong migratory and invasive abilities [1]. Although there is increasing research on its invasive and migratory abilities, malignancy remains the major cause of death in NSCLC [2]. To fully understand the underlying mechanisms and signaling pathway activation is important in NSCLC as to identification of novel treatments that target tumor proliferation.

Chemokine receptors, G-protein-coupled receptors found predominantly on the surface of leukocytes, are associated with the development of multiple cancers [3]. CCR10 is a chemokine receptor usually expressed through melanocytes, plasmacytes, skin-homing T lymphocytes [4], and CCL27 (CCL28)-stimulated cells [5]. CCR10 is expressed in various cancers, and its role in cancer has been widely studied. Due to the expression of CCL27 (its ligand) in the epidermis, the effect of CCR10 in metastasis was initially proposed [6]. Previous data indicate that CCR10/CCL27 acts as the immune escape factor of cancer cells relating to cancer progression [7, 8]. For example, the CCR10-CCL27 interaction plays a crucial role in T-cell homing in inflamed skin [9, 10]. CCR10 is overexpressed in malignant melanoma, and the interaction between CCL27 and CCR10 accelerates melanoma growth and metastasis [7, 11]. However, the effect of activated CCR10 in the multiplication and metastasis of NSCLC cells remains unclear.

This study aimed to assess the expression ratio of CCR10 chemokine-receptor mRNA in patient specimens and human NSCLC cell lines. In par-

Table 1. Clinical characteristics of patients

Characteristics	N	CCR10 expression (M ± SD)	*T*	*P*
Gender				
Male	18	1.8714 ± 0.3014	-0.902	0.381
Female	12	1.7903 ± 0.2962		
Age				
< 60	13	1.5847 ± 0.1352	0.068	0.849
≥ 60	17	1.5793 ± 0.1361		
Histological classification				
AD	21	1.7258 ± 0.1637	2.304	0.038*
SCC	9	1.6156 ± 0.2263		
Differences				
Good + Not bad	18	1.5148 ± 0.1267	-1.647	0.179
Weak	12	1.5402 ± 0.2603		
Metastasis				
Yes	12	1.7238 ± 0.1126	2.593	0.027*
No	18	1.6382 ± 0.1058		
TNM				
I + II	19	1.9603 ± 0.1227	-2.350	0.013*
III + IV	11	1.8974 ± 0.1243		

*: P < 0.05.

ticular, we aimed to evaluate the underlying predictive value of crosstalk between CCR10-CCL27 in the growth and metastasis of NSCLC cell lines, and analyze the relative signal pathway of various molecules in NSCLC cell lines, such as VEGF-C/D, MMP-2/9, and TIMP-1/2, which are known to be regulated by PI3K/Akt sensors.

Materials and methods

Patients

This study included 30 patients with NSCLC (**Table 1**) aged 38-63 years (mean: 56 years). Pathologic clinical data were acquired from medical records. Relevant tissues around the NSCLC tumor were obtained from at least 1 cm around the tumor. All cases underwent pneumonectomy at the Affiliated Hospital of Qingdao University and Baotou Cancer Hospital from September 2015 to April 2017 and were randomly chosen. The local Ethics Committee of the affiliated hospital of Qingdao University provided approval for this study (Approval number: NCT01563872). All specimens in this study were used with the written informed consent of subjects and clinicians. All specimens underwent reexamination and were diagnosed by two pathological doctors.

Cells

Six cell specimens of NSCLC cell strains (A549, SPC-A1, NCI-H1975, NCI-H1299, NCI-H1650, and SK-MES-1) were bought in the Institute of Biochemistry and Cell Biology, Chinese Academy of Sciences. The cell specimens were incubated at 37°C with 5% CO_2 in RPMI-1640 or DMEM medium (10% fetal bovine serum, 100 U/ml PCN, 100 mg/ml SM). The cells were cultured in 100 ng/ml of CCL27 for 2 days between performing different tests. For wortmannin treatment, the cells were firstly cultured with 100 ng/ml of CCL27 for 36 h, and then treated with 5 nM wortmannin for 12 h.

CCK8 assay

The growth of NSCLC cells was measured using the Cell Counting Kit-8 (CCK-8) in a 96-well plate based on the standard procedure in manufacturer's instructions. Briefly, cells with 5×10^3 cells/well in quantity were inoculated in a 96-well plate and cultured until 80% confluence was obtained. CCK-8 was added to each well after 0, 24, 48, and 72 h of transfection. After 1 h of incubation, cellular viability was detected by measuring the absorbance of the dye at 450 nm.

MTT method

The MTT method was performed to evaluate viability. In short, the cell specimens were stimulated in 0.5 mg/mL of methyl thiazolyl tetrazolium (20 μL), and the supernatant was discarded later. Subsequently, dimethylsulfoxide (150 μL) was poured into each well and rotated for 10 min, dissolving the formaldehyde dye. Finally, the absorbance was detected at 540 nm using an Infinite 200 Micro-plate Reader (Tecan, Männedorf, Switzerland).

Colony formation assay

Two days after CCL27 treatment, the cells that have been transfected were suspended in 8 mL of 0.4% top agar with RPMI-1640/DMEM including 10% fetal bovine serum, and placed in 12-well plate containing 0.5% bottom-layer

agar (0.5 mL). Following 14-day culture, 3 wells of each plate were randomly selected to count the number of visible colonies.

Transwell migration assays

Two days after CCL27 treatment, NSCLC cells were lysed using trypsin treatment and rinsed using D-Hanks solution 1 time. To detect the migratory or invasive ability of the cells, culture or matrigel inserts with pore size of 8 μm were placed in culture plates with 24 wells. DMEM/F-12 culture liquid (400 μL) including 10% fetal bovine serum and 20 ng/ml hepatocyte growth factor were added in the lower part of transwell chamber. Next, the cells (1×10^5 cells/ml) were placed in the higher chamber to incubate for 20 h, and the migration of cells stained with crystal violet in the pores was observed under the microscope.

Wound-healing assay

A 10-μL pipette tip was used to scrape the confluent cells in 6-well plates. After the cells migrating to the wound were fixed, the scratched area was detected under a microscope. Migration ratio (%) was obtained by dividing the 48-h width by the 0-h width.

Western blotting

Cell specimens were dissolved using the RIPA buffer (50 mM Tris-HCl, 150 mM NaCl, 1% NP-40, 0.1% SDS, pH 8.0) after adding proteinase restrainer. The protein consistencies were detected using the bicinchoninic acid Protein Quantitation Kit. The protein specimen was electroblotted onto PVDF membranes with pore sizes of 0.45 after 10% SDS-PAGE separation. The cytomembranes were blocked in PBST with 5% BSA for 1 h at room temperature and cultured overnight at 4°C with the corresponding primary antibodies, including anti-GAPDH (1:5000, ab9485, Abcam), anti-TIMP-1 (1:500, ab61224, Abcam), anti-TIMP-2 (1:1000, ab1828, Abcam), anti-MMP-2 (1:1000, ab86607, Abcam), anti-MMP-9 (1:1000, ab38898, Abcam), anti-VEGF-C (1:2000, ab9546, Abcam), anti-VEGF-D (1:1000, ab95542, Abcam), anti-PI3K (1:1000, ab86714, Abcam), anti-Akt (1:2000, ab8805, Abcam), and anti-p-Akt (1:1000, ab38449, Abcam). The secondary antibody of Amersham ECL peroxidase, including goat anti-mouse IgG (1:10000, A0216, Beyotime) and goat anti-rabbit IgG (1:10000, A0208, Beyotime), was cultured with the membranes at room temperature for 1 h. Western blotting immunoreactivity was measured using the SuperSignal West Femto Maximum Sensitivity Substrate Kit (Thermo) and C-DiGit Blot Scanner.

RNA extraction with real-time quantitative polymerase chain reaction (Q-PCR) method

RNA was extracted differently from treatment-stimulated NSCLC cells and TRIzol reagent-treated cardiac tissues based on the manufacturer's protocol. miR-506 expression was detected using the LightCycler®480 (Roche, Germany), and GAPDH was used as an intrinsic control. Q-PCR (20 μL) was performed using SYBR Green PCR Master Mix at 95°C for 10 min, and 40 cycles at 95°C for 15 s, 60°C for 30 s, and 72°C for 30 s using the Lightcycle 480 high throughput real-time fluorescent quantitative PCR instrument. The ($2^{-\Delta\Delta CT}$) target amount was acquired through the standardization of intrinsic reference, and data associated with a calibrating instrument (means of the controls). Primer sequences used for Q-PCR were displayed as follows: CCR10 F: 5'-CAG CCT TAT TCC TGG CAT GT-3', CCR10 R: 5'-CTT GCA AAC TGC CTG ACA TT-3'; VEGF-C F: 5'-TGC CGA TGC ATG TCT AAA CT-3', VEGF-C R: 5'-TGA ACA GGT CTC TTC ATC CAG C-3'; VEGF-D F: 5'-GTA TGG ACT CTC GCT CAG CAT-3', VEGF-C R: 5'-AGG CTC TCT TCA TTG CAA CAG-3'; MMP-2 F: 5'-AGC GAG TGG ATG CCG CCT TTA A-3', MMP-2 R: 5'-CAT TCC AGG CAT CTG CGA TGA G-3'; MMP-9 F: 5'-GCT GAC TAC GAT AAG GAC GGC A-3', MMP-9 R: 5'-TAG TGG TGC AGG CAG AGT AGG A-3'; TIMP-1 F: 5'-CAT CCT GTT GTT GCT GTG GCT GAT-3', TIMP-1 R: 5'-GTC ATC TTG ATC TCA TAA CGC TGG-3'; TIMP-2 F: 5'-CTC GCT GGA CGT TGG AGG AAA GAA-3', TIMP-2 R: 5'-AGC CCA TCT GGT ACC TGT GGT TCA-3'; PI3K F: 5'-CTC TCC TGT GCT GGC TAC TGT-3', PI3K R: 5'-GCT CTC GGT TGA TTC CAA ACT-3'; Akt F: 5'-ATC CCC TCA ACA ACT TCT CAG T-3', Akt R: 5'-CTT CCG TCC ACT CTT CTC TTT C-3'; GAPDH F: 5'-CCT GAG GCT CTT TTC CAG CC-3', GAPDH R: 5'-TAG AGG TCT TTA CGG ATG TCA-3'.

Statistical analysis

Results are expressed as mean ± SD. Comparison among multiple groups and between two groups were analyzed by one-way analysis

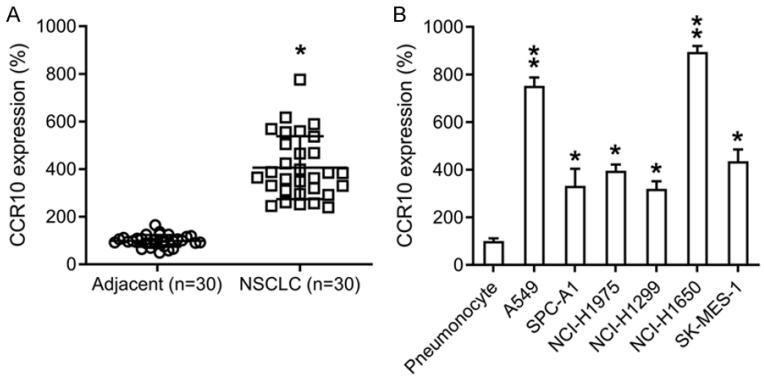

Figure 1. Express level of CCR10 in NSCLC specimens and cell lines. A. Q-PCR showed the expression of CCR10 in NSCLC cancers (N = 30) vs. that in paracancerous healthy tissue (N = 30). B. Q-PCR showed the expression of CCR10 in non-neoplastic lung cells vs NSCLC cell strains (A549, SPC-A1, NCI-H1975, NCI-H1299, NCI-H1650, and SK-MES-1). The differences were significant ($P < 0.05$, $P < 0.01$).

of variance analysis (ANOVA) with Tukey post hoc test and 2-tailed Students' t-test, respectively. SPSS 18.0 and Graphpad (9.0) were used to perform statistical analysis. Differences were significant when $P < 0.05$.

Results

CCR10 expression was increased in NSCLC samples and cells

To probe the effect of CCR10 in the progression of NSCLC, we investigated the expression pattern of CCR10 in 30 patients with NSCLC. In 30 NSCLC tissues, CCR10 level was more upregulated than the adjacent normal healthy hepatic specimens (**Figure 1A**). Subsequently, we detected normal levels of CCR10 in pneumocytes and cancer cell strains (A549, SPC-A1, NCI-H1975, NCI-H1299, NCI-H1650, and SK-MES-1) using Q-PCR. It suggested that the mRNA expression of CCR10 was accelerated in 6 cell strains compared with pneumocytes, especially in cells (A549, SK-MES-1 cells) (**Figure 1B**). The findings showed that CCR10 may have positive affect in the development of NSCLC.

CCR10 activation increased cell growth and multiplication in NSCLC cancer

For detecting the function of CCR10 in NSCLC cell growth and proliferation, cells (A549, SK-MES-1) were induced using 100 ng/ml of CCL27 (ligand of CCR10) and underwent colony formation, CCK-8, and MTT assays. Colony formation assay showed that the addition of CCL27 in cell culture caused a significant increase in the number of cells at 48 h posttreatment, whereas the addition of anti-CCR10 antibody abated the effect of CCL27 in all cells (A549, SK-MES-1) (**Figure 2A**, **2B**). The MTT test was used to evaluate the viability following 48 h CCL27 stimulation therapy. NSCLC cell viability was increased by approximately 75% and 100% in the control and CCL27 treatment groups, respectively. The incubation of anti-CCR10 antibody impaired the cell viability (A549, SK-MES-1) (**Figure 2C**, **2D**). Furthermore, CCK-8 assay was used to estimate cell multiplication (A549, SK-MES-1). Compared with the control group, CCR10 activation upregulated the multiplication of cells (A549, SK-MES-1) at 0, 24, 48, and 72 h after incubation, but the blockage of CCR10 by anti-CCR10 antibody reversed the effect of CCL27 (**Figure 2E**, **2F**). In total, these data suggested that CCR10 activation displayed a simulative effect on cell viability and proliferation of cells via crosstalk with CCL27.

CCR10 activation promotes the invasive and migratory abilities of NSCLC cells

To measure the function of CCR10 in invasive and migratory abilities of NSCLC cells, the cells (A549, SK-MES-1) were induced using 100 ng/ml CCL27 (CCR10 ligand) and underwent wound-healing and transwell migration assays. CCL27 treatment promoted the migration of cells (A549, SK-MES-1), but receptor blockage of CCR10 reduced the migratory rate of cells (A549, SK-MES-1) by wound-healing assay (**Figure 3A**, **3B**). We also found that CCR10 activation enhanced the invasion of cells (A549, SK-MES-1); however, CCR10 blockage completely reversed the effect of CCL27 stimulation (**Figure 3C**, **3D**).

CCR10 activation increases the levels of VEGF-C/D, MMP-2/9, and TIMP-1/2

VEGF-C/D, MMP-2/9, and TIMP-1/2 are widely known as key regulators of cancer metastasis [12, 13]; therefore, we assessed the expres-

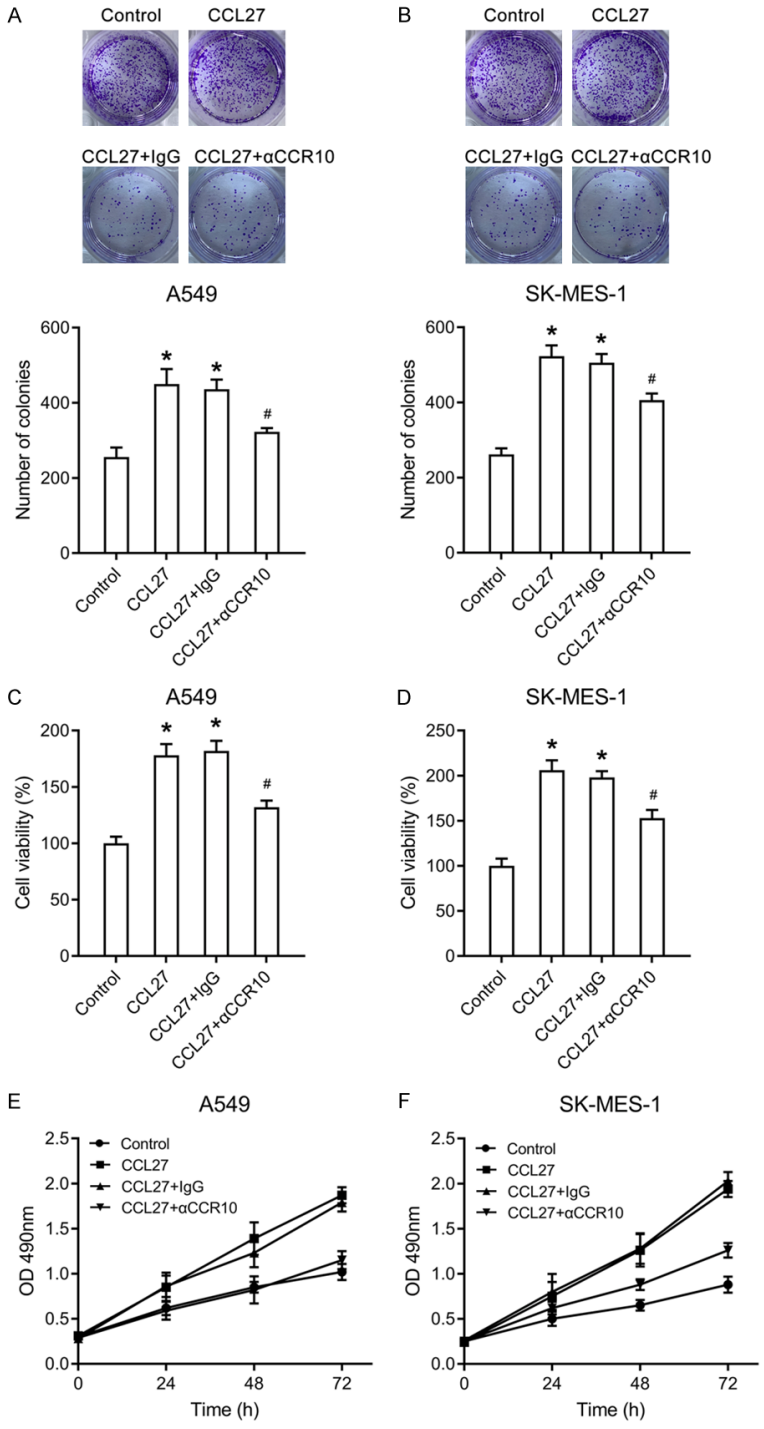

Figure 2. Role of CCR10 activation in NSCLC cell viability and multiplication. Cells (A549 and SK-MES-1) were stimulated in 100 ng/ml CCL27 and/or anti-CCR10 antibody for 48 h. A, B. Multiplication of cells (A549, SK-MES-1) was measured 48 h after CCL27 treatment by colony formation assay. C, D. The NSCLC viability was detected through MTT method 48 h post treatment. E, F. At 24, 48, and 72 h post treatment, the multiplication of cancer cells was decided through CCK-8 assays. Compared with Control group, the difference was significant ($P < 0.05$); Compared with CCL27 group, the difference was significant ($P < 0.05$).

sion of these 6 regulators in cells (A549, SK-MES-1) following CCL27 stimulation at both levels of mRNA and protein, using QRT-PCR and western blotting analyses. Western blotting results clearly demonstrated that the expression of VEGF-C/D, MMP-2/9, and TIMP-1/2 was increased after CCL27 stimulation, whereas this increment was because of the use of CCR10 antibody (**Figure 4A**, **4B**). Meanwhile, QRT-PCR data indicated a similar trend for mRNA expression of 6 regulators in all cells (A549 and SK-MES-1) (**Figure 4C**, **4D**). The results suggested that CCR10 activation promotes the expressions of VEGF-C/D, MMP-2/9, and TIMP-1/2.

CCL27 stimulation activated the PI3K/Akt signal transduction

Previous studies have suggested that the activated PI3K/Akt signal pathway was closely related to the upregulation of VEGF-C/D, MMP-2/9, and TIMP-1/2 in NSCLC [14-16]. Furthermore, we determined the expression and phosphorylation of PI3K and Akt using western and QRT-PCR. Western blotting indicated that the expression of PI3K and phosphorylated Akt in cells (A549 and SK-MES-1) increased following CCL27 stimulation, whereas the inhibition of CCR10 reversed the activation of PI3K and Akt pathway. Akt expression levels were unchanged after different treatments (**Figure 5A**, **5B**). QRT-PCR also suggested that PI3K mRNA expression was upregulated via CCL27 treatment, but decreased af-

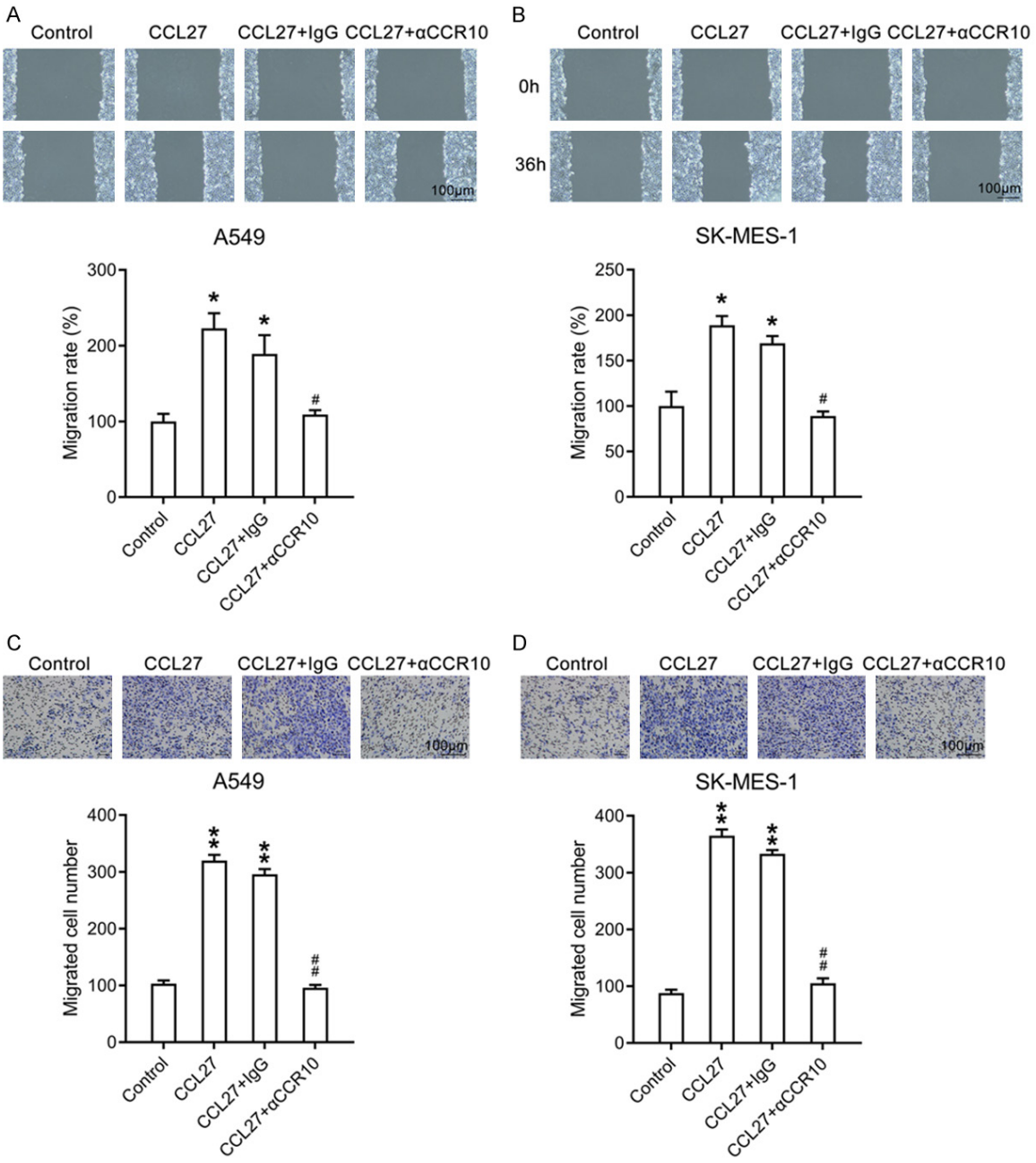

Figure 3. CCR10 activation promoted migratory and invasive ability of NSCLC cells. Cells (A549, SK-MES-1) were stimulated by 100 ng/ml CCL27 and (or) anti-CCR10 antibody for 48 h. A, B. Migratory capability of cells (A549 and SK-MES-1) were detected through wound-healing assay. C, D. Transwell migration assay was carried out to determine the invasive capability of A549 and SK-MES-1 cells. Compared with Control group, the differences were significant ($P < 0.05$, $P < 0.01$); compared with CCL27 group, the differences were significant ($P < 0.05$, $P < 0.01$).

ter the addition of CCR10 antibody; however, the Akt levels were not altered (**Figure 5C**, **5D**).

Inhibition of PI3K activity counteracted the role of CCL27 stimulation in cell multiplication and metastasis of NSCLC patients

Knowing that PI3K/Akt signal pathway was related to the expressed VEGF-C/D, MMP-2/9, and TIMP-1/2 in NSCLC [14-16], coupled with our data confirming that this pathway was activated in cells (A549 and SK-MES-1), this pathway was blocked using wortmannin treatment. The downregulation of Akt phosphorylation clearly indicated the successful inhibition of this pathway in all cells of A549 and SK-MES-1 by wortmannin, even though the expressed

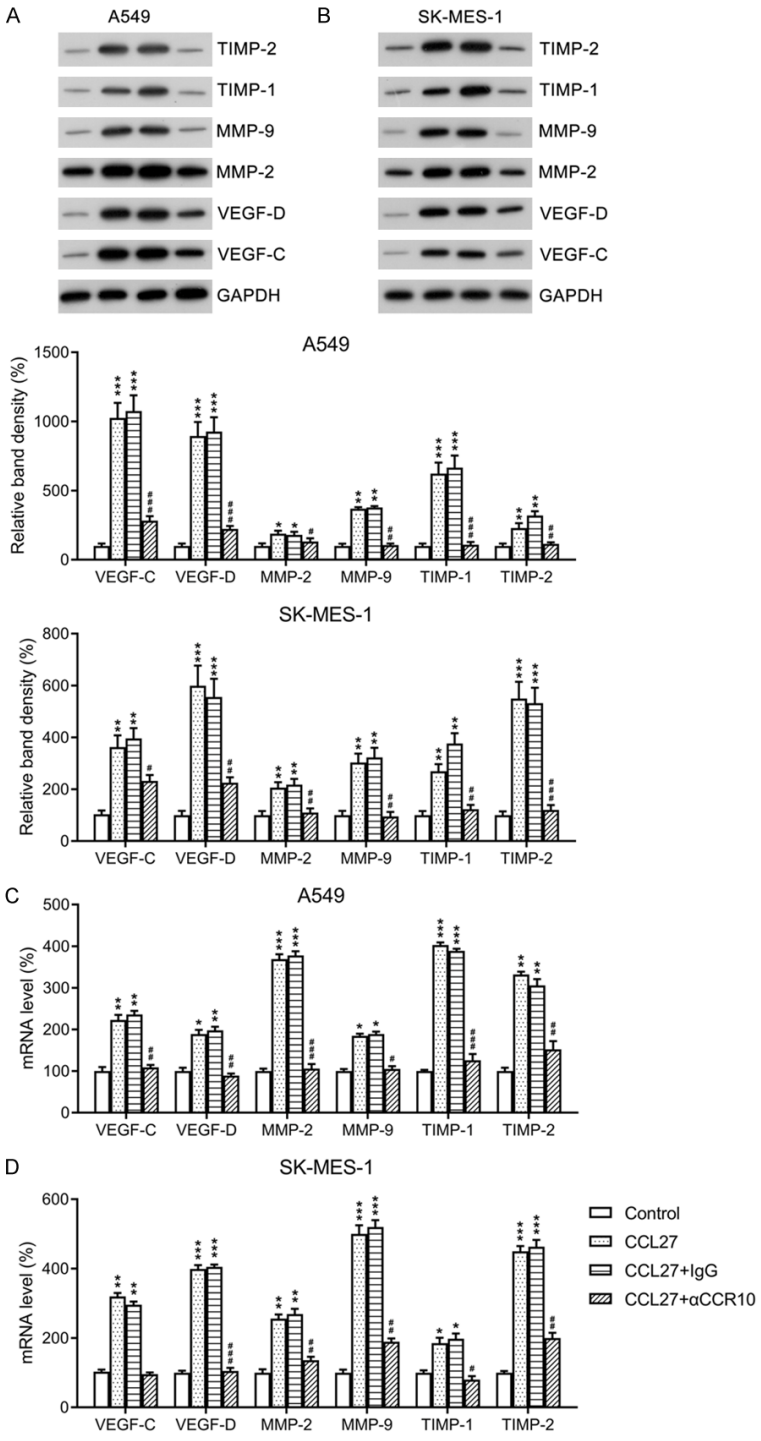

Figure 4. CCR10 activation regulated the level of gene related to cancer metastasis. Cells (A549, SK-MES-1) were stimulated by 100 ng/ml CCL27 and (or) anti-CCR10 antibody for 48 h. A, B. WB were used to estimate the expressive VEGF-C/D, MMP-2/9, and TIMP-1/2 in protein level in A549 and SK-MES-1 cells. C, D. Q-PCR was used to examine the VEGF-C/D, MMP-2/9, and TIMP-1/2 in mRNA level in A549 and SK-MES-1 cells. Compared with Control group, the differences were significant ($P < 0.05$, $P < 0.01$, $P < 0.001$); compared with CCL27 group, the differences were significant ($P < 0.05$, $P < 0.01$, $P < 0.001$).

PI3K and Akt were not changed (**Figure 6A**, **6B**). WB data also indicated that expressed VEGF-C/D, MMP-2/9, and TIMP-1/2 decreased after PI3K inhibition in cells (A549, SK-MES-1) (**Figure 6A**, **6B**).

Colony formation was performed to assess cell growth after PI3K inhibition. The results showed that number of generated colonies was significantly reduced due to PI3K inhibition in CCL27-stimulated cells (A549, SK-MES-1) (**Figure 7A**, **7B**), suggesting that PI3K/Akt signal pathway was related to the CCL27-accelerated development of cells (A549, SK-MES-1).

Moreover, PI3K deactivation remarkably reduced the migration of CCR10-actived cells (A549, SK-MES-1), through the demonstration of wound-healing method (**Figure 7C**, **7D**). Meanwhile, PI3K inhibition also led to an obvious reduction in the amount of invasive A549 and SK-MES-1 cells following wortmannin, using transwell assay (**Figure 7E**, **7F**). Thus, PI3K/Akt signal pathway also participated in the CCL27-stimulated cell metastasis (A549, SK-MES-1).

Discussion

Molecular mechanisms facilitate tumor metastasis and serve as a major measure for prediction and therapeutic prevention of malignant melanoma metastasis. Previous studies have examined the role of chemokine receptors during tumor proliferation [17]. Differentiation in the growth of chemokine receptors and interaction with ligands has proven to be cru-

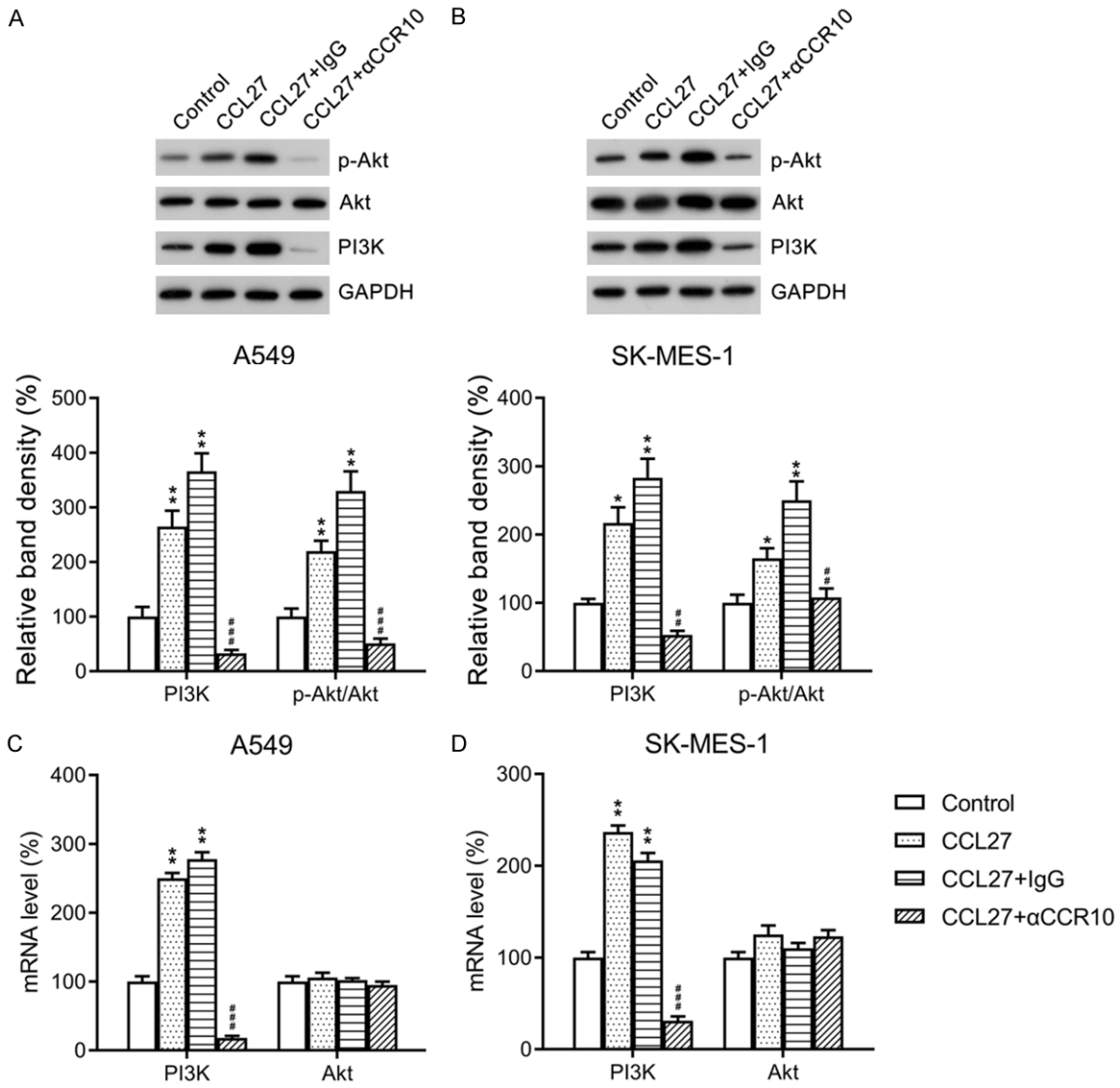

Figure 5. CCR10 activation regulated expression and phosphorylation of PI3K and Akt. Cells (A549, SK-MES-1) were stimulated by 100 ng/ml CCL27 and (or) anti-CCR10 antibody for 48 h. A, B. WB were applied to evaluate the expressed PI3K and Akt, and phosphorylated Akt at protein level in A549 and SK-MES-1 cells. C, D. Q-PCR was used to evaluate the mRNA level of PI3K and Akt in A549 and SK-MES-1 cells. Compared with Control group, the difference was significant ($P < 0.01$); Compared with CCL27 group, the difference was significant ($P < 0.01$, $P < 0.001$).

cial molecular mechanisms leading to local lymph nodes and distant metastasis. More specifically, a role of CCR10 in the development of tumors has been demonstrated [18, 19]. The present data demonstrated that crosstalk between CCR10, which had high expression levels in NSCLC specimens and cell lines, and CCL27 promote viability, multiplication, migration, and invasion of cells (A549 and SK-MES-1), which could be reversed using anti-CCR10 antibody. Moreover, CCR10 activation increased the expression of metastasis-related VEGF-C/D, MMP-2/9, and TIMP-1/2, and promoted the activation of PI3K-Akt pathway. Furthermore, PI3K inhibition by wortmannin inhibited the expression of VEGF-C/D, MMP-2/9, and TIMP-1/2, and antagonized the influence of CCL27 stimulation in cell (A549 and SK-MES-1) viability and metastasis. In brief, this information suggested an interaction between CCR10 and CCL27 that affects the properties of NSCLC cell lines.

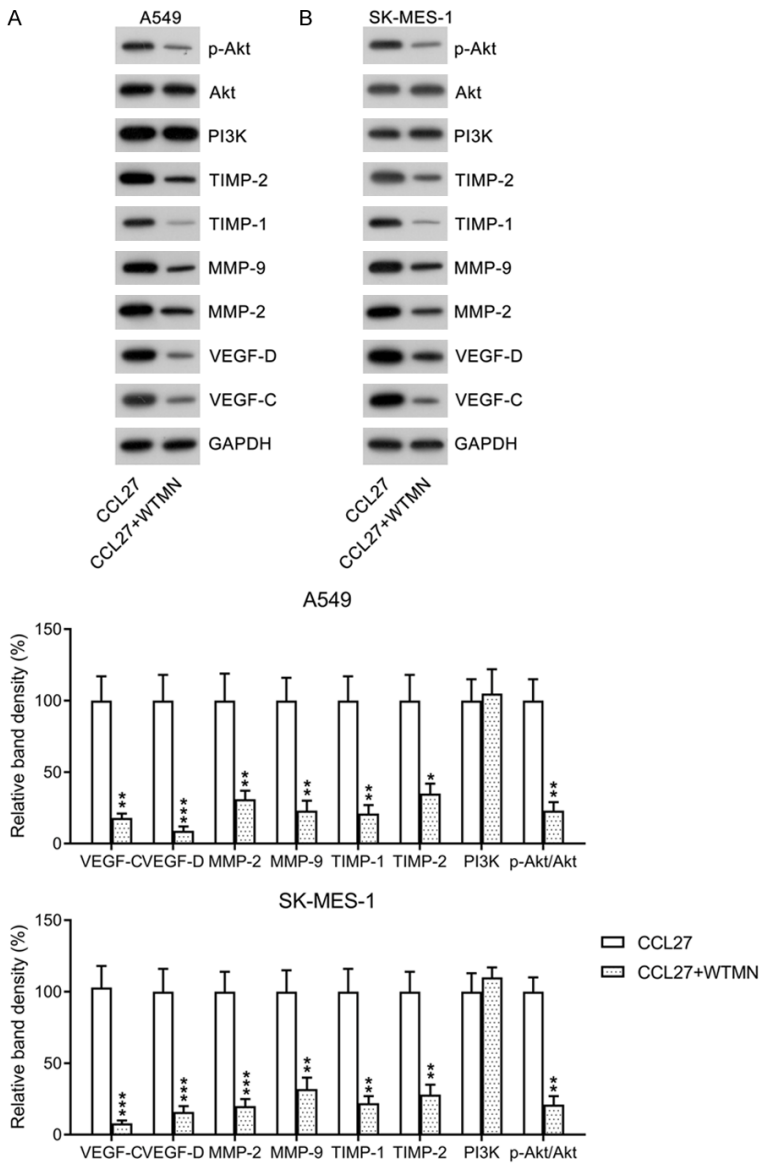

Figure 6. Wortmannin administration reduced growth and metastasis of CCL27-stimulated NSCLC cells. Cells (A549, SK-MES-1) were stimulated by 100ng/ml of CCL27 and (or) 2 μM Wortmannin (WTMN) for 48 h. WB was used to evaluate the expressed VEGF-C/D, MMP-2/9, TIMP-1/2, PI3K and Akt, as well as phosphorylated Akt at protein level in (A) A549 and (B) SK-MES-1 cells. Compared with CCL27 group, the difference was signifcant ($P < 0.01$).

Kai et al. found that CCR10 was overexpressed in SCC [20]. Kuehnelt-Leddihn et al. proposed that the overexpression of CCR10 in primary human cutaneous melanoma was associated with worsening melanoma prognosis [21]. In malignant melanomas, T lymphocyte density was significantly decreased from thin melanomas to intermediate and thick ones. CCR10 expression was found both in benign and malignant lesions and it was directly correlated with the Breslow depth and inversely with T lymphocyte density [7]. Chen et al. reported that chemokine receptor CCR10 is highly expressed in human glioblastoma compared with control brain tissue. In vitro, signaling through CCL27-CCR10 mediates activation of p-Akt, and subsequently induces proliferation and invasive responses. Cell proliferation and invasion promoted by CCL27 were blocked by inhibition of p-Akt or CCR10 [22]. In breast cancer, CCR10 expression was found upregulated in breast cancer cells and tissues. CCL27/CCR10 axis promoted breast cancer cell invasion and migration via increasing MMP-7 expression and inducing ERK1/2 activation [11]. These studies have demonstrated an oncogenic function of CCR10 on the malignancies. This research showed an increased expression of CCR10 in NSCLC cell lines. Moreover, we found that CCR10 expression and activation by CCL27 were associated with proliferation, invasion, and migration. These results showed that CCR10 and CCL27 may be associated with NSCLC cell invasion and metastasis.

Intracellular signal mediated by chemokine receptors depends on adjacent G-proteins. Some signal molecules associated with the activated chemokine receptors contain Akt, protein kinase (MAPK and PI3K) activated by ERK1/2 mitogen, STAT3, and NFkB. However, few studies reported on the downstream signal pathways regulated by CCL27-CCR10 interaction in NSCLC. PI3K/Akt signal pathway was upregulated in CCL27 and CCR10 specimens and played a key role in cell multiplication, migration, and survival [23, 24]. In malignant melanoma and glioma, CCR10 accelerates cell multiplication via activated PI3K/Akt pathway

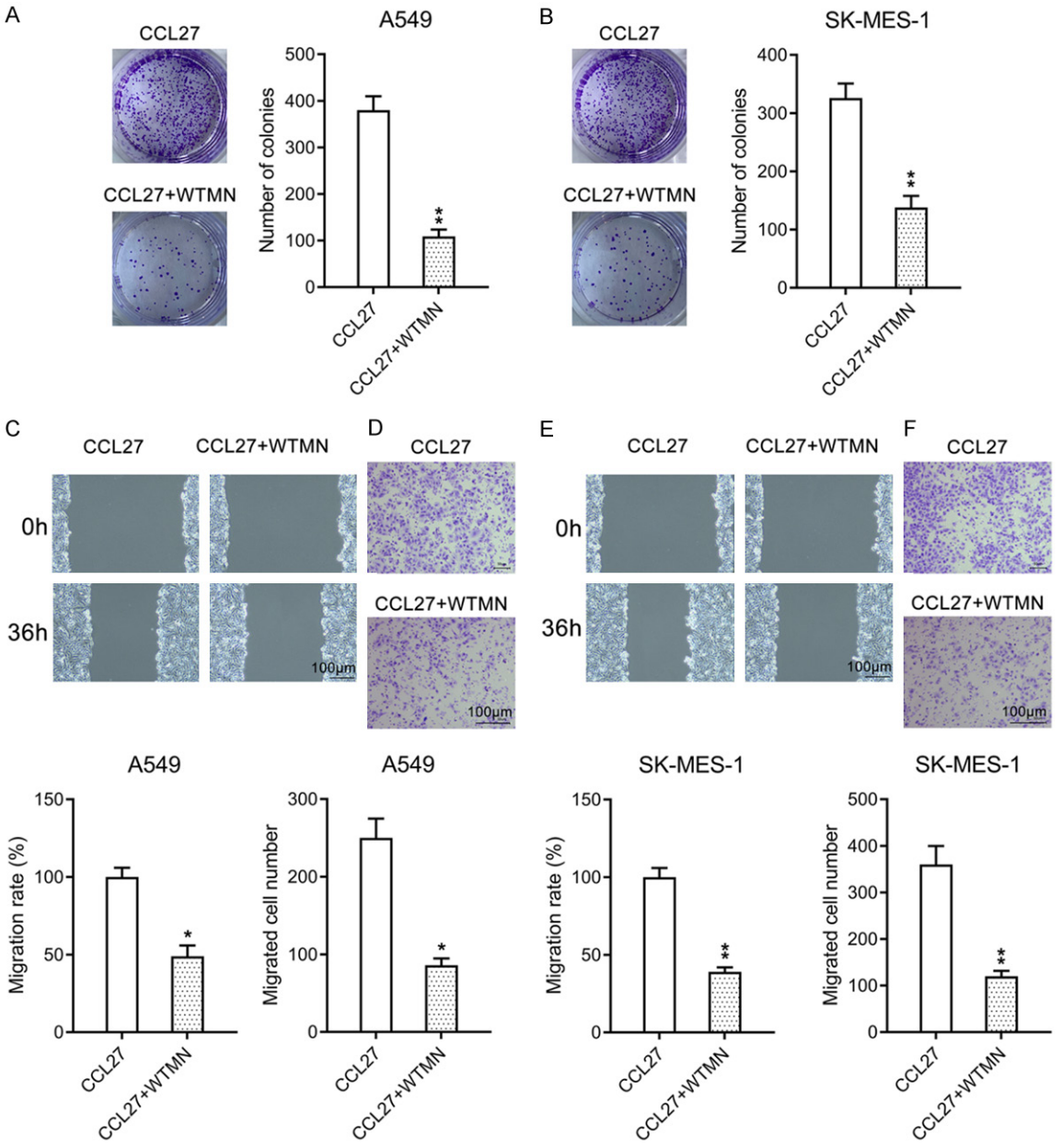

Figure 7. Wortmannin administration reduced the expression of gene related to cancer metastasis and PI3K/Akt pathway. Cells (A549, SK-MES-1) were stimulated by 100 ng/ml of CCL27 and (or) 2 μM Wortmannin (WTMN) for 48 h. Growth of (A) A549 and (B) SK-MES-1 cells was measured 48 h after CCL27 treatment by colony formation assay. Wound healing assay were performed to detect the migration of (C) A549 cells. Invasive ability of (D) A549 cells was measured by transwell migration assay. Wound healing assay were performed to detect the migration of (E) SK-MES-1 cells. Invasive ability of (F) SK-MES-1 cells was measured by transwell migration assay. Compared with CCL27 treatment group, the difference was statistically signifcant ($P < 0.01$).

[22]. In hepatocellular carcinoma, phosphorylated Akt has also proven to act as a crucial factor in carcinogenesis, and p-Akt level is actively related to poor prognosis in HCC patients. Meanwhile, expressed CCR10 obviously increased the phosphorylated hepatocellular Akt [25, 26]. In the current study, PI3K/Akt signal pathway was activated via crosstalk between CCR10 and CCL27 in cancer cell lines, A549 and SK-MES-1 cells. To assess the participation of PI3K/Akt during CCL27 and CCR10 mediated migration of NSCLC cells, PI3K inhibitor Wortmannin was applied to treat cells [27]. The management of wortmannin, causing dephosphorylation of Akt, antagonized the influence of CCL27 stimu-

lation in cell viability and metastasis, suggesting that PI3K/Akt participated in the multiplication and migration of tumor cells.

In short, this study shows high expression of CCR10 in NSCLC cells. CCR10 expression is related to growth, multiplication, migration, and invasion of NSCLC cells. CCR10 activation by CCL27 can lead to the generation and activation of PI3K/Akt, improve the level of VEGF-C/D, MMP-2/9, and TIMP-1/2 production, and participate in invasive and migratory characteristics of NSCLC cells.

Disclosure of conflict of interest

None.

Address correspondence to: Biyuan Zhang, Department of Radiation Oncology, The affiliated Hospital of Qingdao University, No. 16, Jiangsu Road, Qingdao 266003, Shandong, China. Tel: +86-18661807926; E-mail: byzhang_2006@126.com

References

[1] Siegel R, Naishadham D and Jemal A. Cancer statistics, 2012. CA Cancer J Clin 2012; 62: 10-29.

[2] Thomson CS and Forman D. Cancer survival in England and the influence of early diagnosis: what can we learn from recent EUROCARE results? Br J Cancer 2009; 101 Suppl 2: S102-109.

[3] Mantovani A, Savino B, Locati M, Zammataro L, Allavena P and Bonecchi R. The chemokine system in cancer biology and therapy. Cytokine Growth Factor Rev 2010; 21: 27-39.

[4] Moed H, Boorsma DM, Tensen CP, Flier J, Jonker MJ, Stoof TJ, von Blomberg BME, Bruynzeel DP, Scheper RJ and Rustemeyer T. Increased CCL27-CCR10 expression in allergic contact dermatitis: implications for local skin memory. J Pathol 2004; 204: 39-46.

[5] Xiong N, Fu Y, Hu S, Xia M and Yang J. CCR10 and its ligands in regulation of epithelial immunity and diseases. Protein Cell 2012; 3: 571-580.

[6] Monteagudo C, Ramos D, Pellín-Carcelén A, Gil R, Callaghan RC, Martín JM, Alonso V, Murgui A, Navarro L and Calabuig S. CCL27-CCR10 and CXCL12-CXCR4 chemokine ligand-receptor mRNA expression ratio: new predictive factors of tumor progression in cutaneous malignant melanoma. Clin Exp Metastasis 2012; 29: 625-637.

[7] Simonetti O, Goteri G, Lucarini G, Filosa A, Pieramici T, Rubini C, Biagini G and Offidani A. Potential role of CCL27 and CCR10 expression in melanoma progression and immune escape. Eur J Cancer 2006; 42: 1181-1187.

[8] Pivarcsi A, Müller A, Hippe A, Rieker J, Van Lierop A, Steinhoff M, Seeliger S, Kubitza R, Pippirs U and Meller S. Tumor immune escape by the loss of homeostatic chemokine expression. Proc Natl Acad Sci U S A 2007; 104: 19055-19060.

[9] Faaij CM, Lankester AC, Spierings E, Hoogeboom M, Bowman EP, Bierings M, Révész T, Egeler RM, Van Tol MJ and Annels NE. A possible role for CCL27/CTACK-CCR10 interaction in recruiting CD4+ T cells to skin in human graft-versus-host disease. Br J Haematol 2006; 133: 538-549.

[10] Homey B, Alenius H, Müller A, Soto H, Bowman EP, Yuan W, McEvoy L, Lauerma AI, Assmann T and Bünemann E. CCL27-CCR10 interactions regulate T cell-mediated skin inflammation. Nat Med 2002; 8: 157-165.

[11] Lin HY, Sun SM, Lu XF, Chen PY, Chen CF, Liang WQ and Peng CY. CCR10 activation stimulates the invasion and migration of breast cancer cells through the ERK1/2/MMP-7 signaling pathway. Int Immunopharmacol 2017; 51: 124-130.

[12] Groblewska M, Mroczko B, Gryko M, Pryczynicz A, Guzińska-Ustymowicz K, Kędra B, Kemona A and Szmitkowski M. Serum levels and tissue expression of matrix metalloproteinase 2 (MMP-2) and tissue inhibitor of metalloproteinases 2 (TIMP-2) in colorectal cancer patients. Tumour Biol 2014; 35: 3793-3802.

[13] Takizawa H, Kondo K, Fujino H, Kenzaki K, Miyoshi T, Sakiyama S and Tangoku A. The balance of VEGF-C and VEGFR-3 mRNA is a predictor of lymph node metastasis in non-small cell lung cancer. Br J Cancer 2006; 95: 75-79.

[14] Fumarola C, Bonelli MA, Petronini PG and Alfieri RR. Targeting PI3K/AKT/mTOR pathway in non small cell lung cancer. Biochem Pharmacol 2014; 90: 197-207.

[15] Cortas T, Eisenberg R, Fu P, Kern J, Patrick L and Dowlati A. Activation state EGFR and STAT-3 as prognostic markers in resected non-small cell lung cancer. Lung Cancer 2007; 55: 349-355.

[16] Tsurutani J, Steinberg SM, Ballas M, Robertson M, LoPiccolo J, Soda H, Kohno S, Egilsson V and Dennis PA. Prognostic significance of clinical factors and Akt activation in patients with bronchioloalveolar carcinoma. Lung Cancer 2007; 55: 115-121.

[17] Vicari AP and Caux C. Chemokines in cancer. Cytokine Growth Factor Rev 2002; 13: 143-154.

[18] Lazennec G and Richmond A. Chemokines and chemokine receptors: new insights into cancer-related inflammation. Trends Mol Med 2010; 16: 133-144.

[19] Richmond A, Yang J and Su Y. The good and the bad of chemokines/chemokine receptors in melanoma. Pigment Cell Melanoma Res 2009; 22: 175-186.
[20] Kai H, Kadono T, Kakinuma T, Tomita M, Ohmatsu H, Asano Y, Tada Y, Sugaya M and Sato S. CCR10 and CCL27 are overexpressed in cutaneous squamous cell carcinoma. Pathol Res Pract 2011; 207: 43-48.
[21] Kühnelt-Leddihn L, Müller H, Eisendle K, Zelger B and Weinlich G. Overexpression of the chemokine receptors CXCR4, CCR7, CCR9, and CCR10 in human primary cutaneous melanoma: a potential prognostic value for CCR7 and CCR10? Arch Dermatol Res 2012; 304: 185-193.
[22] Chen L, Liu X, Zhang H-Y, Du W, Qin Z, Yao Y, Mao Y and Zhou L. Upregulation of chemokine receptor CCR10 is essential for glioma proliferation, invasion and patient survival. Oncotarget 2014; 5: 6576-83.
[23] Dehm SM and Bonham K. SRC gene expression in human cancer: the role of transcriptional activation. Biochem Cell Biol 2004; 82: 263-274.
[24] Yu JC, Li W, Wang LM, Uren A, Pierce JH and Heidaran MA. Differential requirement of a motif within the carboxyl-terminal domain of alpha-platelet-derived growth factor (alpha PDGF) receptor for PDGF focus forming activity chemotaxis, or growth. J Biol Chem 1995; 270: 7033-7036.
[25] Nakanishi K, Sakamoto M, Yamasaki S, Todo S and Hirohashi S. Akt phosphorylation is a risk factor for early disease recurrence and poor prognosis in hepatocellular carcinoma. Cancer 2005; 103: 307-312.
[26] Wu Q, Chen JX, Chen Y, Cai LL, Wang XZ, Guo WH and Zheng JF. The chemokine receptor CCR10 promotes inflammation-driven hepatocarcinogenesis via PI3K/Akt pathway activation. Cell Death Dis 2018; 9: 232.
[27] Abliz A, Deng W, Sun R, Guo W, Zhao L and Wang W. Wortmannin, PI3K/Akt signaling pathway inhibitor, attenuates thyroid injury associated with severe acute pancreatitis in rats. Int J Clin Exp Pathol 2015; 8: 13821-33.